Calculation of n+^{232}Th Reaction Cross Sections in the En≤20 MeV Energy Range

Han Yinlu
China Institute of Atomic Energy, P.O. Box 275(41), Beijing 102413, China
** e-mail: han@iris.ciae.ac.cn*

Consistent calculation and analysis of neutron scattering data of ^{232}Th with optical model, semiclassical model includes both the Hauser-Feshbach theory and the exciton model, and the coupled channel theory is carried out in the En≤20 MeV energy range based on the experimental data of total, nonelastic-scattering, fission, and other reaction cross section and elastic-scattering angular distributions. Especially, the analysis includes the elastic and inelastic scattering angular distribution, the inelastic scattering cross sections of discrete levels, the prompt fission neutron spectra, the double differential cross section and the angle-integrated spectra for neutron emission. Theoretical calculations are compared with recent experimental data and other evaluated data from ENDF/B6 and JENDL-3.

I.Introduction

The neutron interactions cross sections and prompt fission neutron spectrum in the energy range below 20 MeV are of fundamental importance for fission and accelerator-driven reactors because they dominate the neutron transport and neutron regeneration, respectively. Therefore, precise nuclear reaction data are required for the nuclear and shielding design of fission reactors and accelerator-based system such as accelerator-driven transmutation system. On the other hand, a careful analysis of certain nuclear cross section data file reveals either that various kinds of errors (even clerical ones) are indeed present in the evaluations for ^{232}Th, or that these evaluations are not fully consistent with the most recent and accurate experimental data and results.

To meet needs, accurate nuclear reaction data of common cross sections, number of neutron per fission, the prompt fission neutron spectra, the angle-integrated spectra for neutron emission, neutron-induced double differential cross sections, γ-ray production cross sections andγ-ray production energy spectra for n+^{232}Th reaction are calculated in this work using recent experimental data, various models and methods for the neutron energy region E_n≤20 MeV. The calculated results are analyzed and compared with experimental data and other evaluated data from ENDF/B6 and JENDL-3.

II.Theoretical Model and Parameters

The latest version of the UNF code[1)], which calculates nuclear reaction cross sections at incident neutron energies below 20 MeV, is based on the optical model and the semi-classical model of multistep nuclear reaction processes, including the introduction of formation factors of composite particle in calculations of pick-up type composite particle emissions. Direct inelastic scattering to low-lying levels is calculated using the distorted wave Born approximation and it is included as input into the UNF calculations. The GNASH[2)] code does not have angular momentum conservation in the exciton component, and it uses a semiempirical method for calculating angular distributions in double differential cross sections.

The optical model is used to describe measured total, reaction, elastic scattering cross sections and elastic scattering angular distributions, and to calculate the transmission coefficient of the compound nucleus and the pre-equilibrium emission process. The optical potentials considered here are

Woods-Saxon[3] form for the real part, Woods-Saxon and derivative Woods-Saxon form for the imaginary parts corresponding to the volume and surface absorptions respectively, and the Thomas form for the spin-orbit part. In order to obtain a set of neutron optical potential parameters for ^{232}Th, the optical model code APOM[4] was used in this work. In this code the best neutron optical potential parameters are searched automatically to fit with the relevant experimental data of total cross sections, nonelastic-scattering cross sections, elastic-scattering cross sections, and elastic-scattering angular distributions. The adjustment of optical potential parameters is performed to minimize a quantity called χ^2, which represents the deviation of the theoretical calculated results from the experimental values.

The energy dependencies of potential depths and optimum neutron optical potential parameters of Th are expressed as follows:

$V=51.0445-0.3125E_n+0.008986E_n^2-24.0V_3(N-Z)/A.$

$W_s=7.2421+0.1119E_n-12.0(N-Z)/A.$

U_{so}=6.2

$r_r=1.2386,\ r_s=1.2499,\ r_{so}=1.2386,$

$a_r=0.5932,\ a_s=0.7548,\ a_{so}=0.5932.$

Where Z, N and A are charge, neutron and mass numbers of target, respectively, E_n is incident neutron energy. The units of the potential V, W_s, W_v, U_{so} are in MeV, the lengths r_r, r_s, r_{so}, a_r, a_s, a_{so} are in fermi units and energies E_n is in MeV.

The calculated results of neutron total, nonelastic, elastic scattering cross sections and elastic scattering angular distribution are compared with experimental data for n+^{232}Th reaction. The calculated results of total cross sections are in good agreement with recent experimental data measured at Los Alamos[5] in Fig.1, and elastic scattering angular distribution are in agreement with experimental data, while the calculated results of nonelastic cross sections and elastic scattering cross sections pass through existing experimental data in Fig.2. Based on the above fitting, this set of neutron optical potential parameters is determined for n+^{232}Th reaction.

The direct inelastic scattering cross sections to low-lying states are important in nuclear data theoretical calculations. The code ECIS[6] with a distorted wave Born approximation is used. The discrete levels of ^{232}Th are taken into account from ground (0.0 0^+) up to the twenty-third (1.0787 0^+) excited state. Levels above 1.0787 MeV are assumed to be overlapping and level density formalism to be used. The direct inelastic scattering cross sections and angular distributions of the first four excited levels are calculated. The coupled channel optical model parameters and deformation parameters (β_2=0.1950, β_4 = 0.0820) used in ECIS are taken from Ref.7).

The semiclassical model of multistep nuclear reaction processes, in which the discrete level effect in multiparticle emissions is included as well as the preequilibrium phenomenon combining parity conservation and angular momentum conservation, is used to describe the nuclear reaction preequilibrium and equilibrium decay processes.

This semiclassical model[8] includes both the Hauser-Feshbach theory and the exciton model[9,10], and the exact Pauli exclusion effect in the exciton state densities[11] is taken into account. The pick-up mechanism[12] is used to describe the composite particle emission processes. Based on the leading particle model, the double differential cross section for all kinds of particles is obtained. In order to keep energy conservation for the whole reaction process, the recoil effect is taken into account in the UNF code.

The fission cross section is an important in n+^{232}Th reactions. Fission is included as a decay channel in the UNF code, that is, a fission competitive width can be estimated at every step of the

cascades. Three uncoupled fission barriers are used to represent the fission system. At each barrier a series of transition states characterized by excitation energy above the barrier, spin and parity can be constructed. At higher energies the discrete transition states are replaced by a continuum of such states, using the Gilbert-Cameron level density prescription and appropriate level density enhancement factors. The Bohr-Wheeler theory[13] is used in transmission coefficients computed at each barrier. According to the experimental data of fission cross sections, the adjustment of the height parameters, V_f, the curvature parameters, $\hbar\omega$, of fission barriers, and the saddle level density factors, $K_{1,}$ is performed to minimize a quantity called χ^2, which represents the deviation of the theoretical calculated fission cross sections from the experimental values. The fission parameters obtained, exciton model parameter K and level density parameters are given in Ref.14).

III.Theoretical Results and Analysis

The comparisons of calculated results of (n,γ) reaction cross sections with experimental data are given in Fig.3. The calculated results are in good agreement with experimental data taken from Refs.15-20) in the entire energy region. The calculated results of (n, γ) reaction cross sections are contributions of compound nuclear reaction below 6 MeV, and the direct reaction above 6 MeV. The cross sections of (n, p), (n, d), (n, t) and (n, α) reactions are less than 12 mb, and have no experimental data.

The calculated results of inelastic scattering cross sections and inelastic scattering angular distributions for the first and second excited level are compared with experimental data in Figs.4 to 6. The figures show the compound nuclear reaction is domination for energy below 1.5 MeV, and the direct reaction is domination above 1.5 MeV. The calculated results of inelastic scattering cross sections, and inelastic scattering angular distributions of the first excited level are in good agreement with experimental data[21-23]. The calculated results of inelastic scattering angular distributions of the second excited level are in basically agreement with experimental data. The calculated results of inelastic scattering angular distributions and inelastic scattering cross sections for the first and second excited level are lower than the experimental data at energy 3.4 MeV, and since the experimental data of inelastic scattering angular distribution are high for small angular, the experimental data of inelastic scattering cross section deviates from the tendency of all experimental data.

Since the first, second and third excited state of ^{232}Th are 0.0492, 0.1621 and 0.3332 MeV, it is difficult to distinguish between the elastic scattering and inelastic scattering in experimentally. The experimental data of angular distribution inclusion elastic scattering and inelastic scattering of the first, second and third excited stated were given in Refs.23,24), respectively. The calculated results of elastic, inelastic scattering angular distribution of the first and second excited stated as well as total angular distribution at energy 2.4 MeV and 5.7 MeV are given in Fig.7, the results show the contribution of inelastic scattering are important in total angular distribution. The calculated results are in good agreement with experimental data taken from Ref.23). Fig.8 give the comparisons of calculated results with experimental data for elastic, inelastic scattering angular distribution of the first, second and third excited states in energy from 4.5 to 10 MeV, the calculated results fit experimental data very well for all energy.

Fig.9 gives the comparisons of calculated results with experimental data for (n, n') reaction. The calculated curves pass through the experimental data within error bars. The calculated results for (n, 2n) reaction cross sections are in good agreement with the experimental data taken from Refs.25-29). There is a single experimental datum[30] for the (n, 3n) reaction at E_n=14 MeV, the calculated results are

basically in agreement with the experimental data as shown in Fig.10. The fission cross section obtained from theoretical calculations as shown in Fig.11 and the number of neutrons per fission obtained from the systematic formulism which is obtained according to the experimental data of fission cross sections are modified slightly to better agree with the experimental data. The present results of fission cross section are in good agreement with experimental data[31].

The present calculated results and our earlier data[14] of reaction cross sections for all channels are similar to the evaluated results in ENDF/B6 and JENDL-3 in curve shapes, but fit the new experimental data much better, especially the total cross sections, (n, n'), (n, f) and (n, 2n) reaction cross sections. Based on the agreement of calculated results with experimental data for all reaction cross section, the energy spectrum, double differential cross section, γ-ray production cross sections andγ-ray production energy spectrum are calculated.

The fission neutron spectra are compared with experimental data at 1.5, 2.0, 2.9, 4.1 and 14.7 MeV, the Fig12. shows the theoretical calculated results are in good agreement with experimental data[32-35] for all energy point.

The neutron-induced double differential emission spectra measurement is that of Baba et al.[36] for 1.2, 2.03, 4.25, 6.1, 14.05 MeV incident neutrons. Additionally, Matsuyama et al.[37] gave measurement results at 18.0 MeV. Calculated results and experimental data for neutron double differential emission spectra at 1.2 MeV are shown in Fig.13. Agreement is good over the whole emission energy range. Figure 13 shows some fluctuations in the calculated results, which are from discrete level contribution in the region of 0.15 to 1.1 MeV. The calculated results are the contribution of the fission channel above neutron emission energy 1.35 MeV.

The calculated results have been analyzed and compared to the double differential experiment data in energy 2.03, 4.25, 6.1, 14.05 and 18.0 MeV at Ref.14).

The experimental data and calculated results of angle-integrated neutron emission spectra are compared for incident energy E_n=2.03, 2.6, 4.25, 6.1, 14.05 and 18.0 MeV, respectively. Our results are in excellent agreement with experimental data[36] of angle-integrated neutron emission spectra at 2.03, 4.25 and 14.05 MeV incident energies, and in reasonable agreement with the spectra at 6.1 MeV incident energies. The experimental data of the spectra at 2.6 MeV were also given in Ref.38), Fig.14 is the comparison of calculated results with experimental data at incident energy 2.03 and 2.6 MeV, the calculated results at energy 2.03 MeV are in good agreement with experimental data taken from Ref.36) for the position and height of the peak, and at energy 2.6 MeV, there are some difference between the calculated results and the experimental data taken from Ref.38) for the peak position. The comparison of calculated results with experimental data for energy E_n=4.25 and 6.1 MeV are given in Fig.15. Figs.13 to 15 also show the calculated results are from the contribution of fission spectra above emission neutron energy 2.2, 3.0, 4.5 and 6.4 MeV, the experimental data taken from Ref.36) are in good agreement with calculated results. The comparison of calculated results with experimental data is given in Fig.16 at incident energy 14.05 and 18 MeV. The calculated results are not in agreement with experimental data for $E_{n'}$>5 MeV and $E_{n'}$<14 MeV, where the calculated results are from the contribution of inelastic scattering and (n, 2n) reaction cross sections. Fig.17 gives the contribution of inelastic scattering, (n, 2n), (n, 3n), (n, f) reaction cross sections to spectra, and the values of reaction cross sections are given in table 1 at energy 18 MeV, the cross sections of (n, n'), (n, 3n) and (n, f) reactions are larger than these of (n, 2n) reaction. The calculated spectra for energy 5.0 to 11.0 MeV is reasonable. Figs. 15 and 16 show experimental data of double differential cross sections is inconsistent with those of angle-integrated neutron emission spectra around the elastic peak.

Because emission spectra experimental data of Baba et al. included prompt fission and scattering neutrons, Figs.13 to 16 also demonstrate that calculated results of fission neutron spectra are reasonable.

Since neutron emission spectra and double differential cross sections provide a complementary information on inelastic scattering for discrete and continuum levels, (n, 2n), (n, 3n) reaction and neutron fission reaction of target nucleus, the agreement of neutron emission spectra and double differential cross sections between calculated results and experimental data also shows present calculated results of reaction cross sections are reasonable.

The double differential cross sections for proton, deuteron, triton and alpha emission, γ-ray production cross sections andγ-ray production energy spectrum are also calculated and analyzed at incident neutron energies below 20 MeV. The calculated results are given in our evaluation data file.

All our calculated results have been put into ENDF/B6 format and are saved in the Chinese Evaluated Nuclear Data Library, CENDL.

IV. Conclusion

Based on experimental data of total, nonelastic, elastic scattering cross sections and elastic scattering angular distribution of ^{232}Th, a set of optimal neutron optical potential parameter is obtained by code APOM. All cross sections of neutron induced reactions, angular distributions, double differential cross sections, the angle-integrated spectra, the prompt fission neutron spectra, γ-ray production cross sections andγ-ray production energy spectra are calculated using theoretical models for n+ ^{232}Th at incident neutron energies from 0.05 to 20 MeV, and theoretical calculated results are in good agreement with recent experimental data. The calculated results are given in ENDF/B6 format. The evaluated data of JENDL-3 are recommended for energy En<0.05 MeV.

Acknowledgments

This work is one of the physical and technological researches of Accelerator-Driven clean nuclear Power System (ADS), and supported by the China Ministry of Science and Technology under Contract No. G1999022600. I appreciate greatly the supported of the Researcher Invitation Program to the International Meeting Hosted by the Japan Atomic Energy Research Institute in the Field of Nuclear Safety.

REFERENCES

1) ZHANG Jingshang, Nucl. Sci. Eng. 142,207(2002).

2) P.G. Young, E.D. Arthur, and M.B. Chadwick, Comprehensive Nuclear Model Calculations: Theory and Use of the GNASH Code, Proc. IAEA Workshop Nuclear Reaction Data and Nuclear Reactors-Physics, Design, and Safety, Trieste, Italy, April 15-May 17, 1996, p. 227. A.GANDINI and G. REFFO, Eds., World Scientific Publishing, Ltd., Singapore (1998).

3) F.D. Becchettijr and G.W. Greenlees, Phys. Rev. 182,1190(1969).

4) SHEN Qingbiao, Commun. Nucl. Data Prog., 7,43(1992).

5) W.P. Abfalterer, F.B. Bateman, et al., Phys. Rev, C,63,044608(2001).

6) J. Raynal, “Notes on ECIS94”,CEA-N-2772, p.1, Commissariat a l’Energie Atomique, Saclay, France (1994).

7) G. Vladuca, A. Tudora, M. Sin, Regional Phenomenological Deformed Optical Potential for Neutron Interactions with Actinides, Rom. J. Phys., tome 41, no. 7-8(1996)515-526.

8) ZHANG Jingshang, Nucl. Data Prog., 7,15(1992).
9) G. Mantzouranis, H. Weidenmuller, and D.Agassi, Z. Phys. A,276,145(1976).
10) Z. Sun, S. Wang, J. Zhang, and Y. Zhou, Z. Phys. A,305,61(1982).
11) J. Zhang, and X. Yang, Z. Phys. A,329,69(1988).
12) A. Iwamoto, and K. Harada, Phys. Rev. C,26,1821(1982).
13) D.L. Hill and J.A. Wheeler, Phys. Rev., 89,1102(1953).
14) Han Yinlu, Shen Qingbiao, et al., Nucl. Sci. Eng., to be published.
15) M. Lindner, R.J. Nagle, and J.H. Landrum, Nucl. Sci. Eng. 59,381(1976).
16) W.P. Poenitz and D.L. Smith, Fast Neutron Radioactive Capture Cross Sections. ANL-NDM-42, (1978).
17) K. Kobayashi, Y. Fujita, and N. Yamamuro, Measurement of the Cross Section for the Th-232(n,g) Reaction From 1 KeV to 450 KeV. NEANDC(J)-56/U, (1978).
18) R.P. Anaand, H.M. Jain, et al., Neutron Capture Cross Section of Th-232. BARC-1239, 1984.
19) A.N. Davletshin, E.V. Teplov, et al., Yadernaye Konstanty, 14(1992).
20) A.N. Davletshin, E.V. Teplov, et al., Yadernaye Konstanty,13(1993)
21) N.P. Glazkov, AE, 14,400(1963).
22) G. Haouat, J. Lachkar, et al., Nuc. Sci. Eng., 81,491(1982).
23) T. Iwasaki, M. Baba, et al., Contribution to the Specialists' Meeting on Fast Neutron Scattering on Actinide Nuclei, IWASAKI (1981).
24) A.B. Smith, S. Chiba, Annals of Nuclear Energy, 23,459(1996).
25) R.J. Prestwood, B.P. Bayhurst, Phys. Rev. 121,1438(1961).
26) H. Karius, A. Ackermann, W. Scobel, J. Phys. G,5,715(1979).
27) H. Chatani, I. Kimura, Measurement of Th-232(n, 2n)Th-231 Reaction Cross Section With 14 MeV Neutrons. JAERI-M-91-032, p.245, 1991.
28) H. Chatani, I. Kimura, Annals of Nuclear Energy, 19,477(1992).
29) P. Paics, S. Daroczy, J. Csikai, et al., Phys. Rev. C,32,87(1985).
30) M.H.MC Taggart, H. Goodfellow, J. Nuclear Energy, Parts A&B, Reactor Sci. Technology, AB,17,437(1963).
31) Oleg Shcherbakov, Andrei Donets, et al., J. Nucl. Sci. Tech., Supplement, 2,230(2002).
32) S.E. Sukhikh, G.N. Lovchikova, et al., Yadernaye Konstanty,3,34(1986).
33) M. Baba, H. Wakabayashi, et al., INDC(NDS)-220, 1989.
34) G.S. Boykov, V.D. Dmitriev, et al., Yadernaye Konstanty,53,628(1993).
35) M. Baba, M. Ibaraki, et al., J. Nucl. Sci. Tech., Supplement, 2,204(2002).
36) M. Baba, H. Wakabayashi, T. Ito, et al., Measurements of Prompt Fission Neutron Spectra and Double-Differential Neutron Inelastic Scattering Cross Sections for 238-U and 232-Th. JAERI-M-89-143, 1989.
37) S. Matsuyama, M. Baba, T. Ito, et al., Nucl. Sci. Tech., 27,601(1990).
38) T. Miura, M. Baba, et al., Ann. Nucl. Energy, 28,937(2001).

Table 1 The calculated reaction cross sections at E_n=18 MeV

(n, n')	(n,2n)	(n, 3n)	(n, f)
0.49035	0.27165	1.72164	0.50407

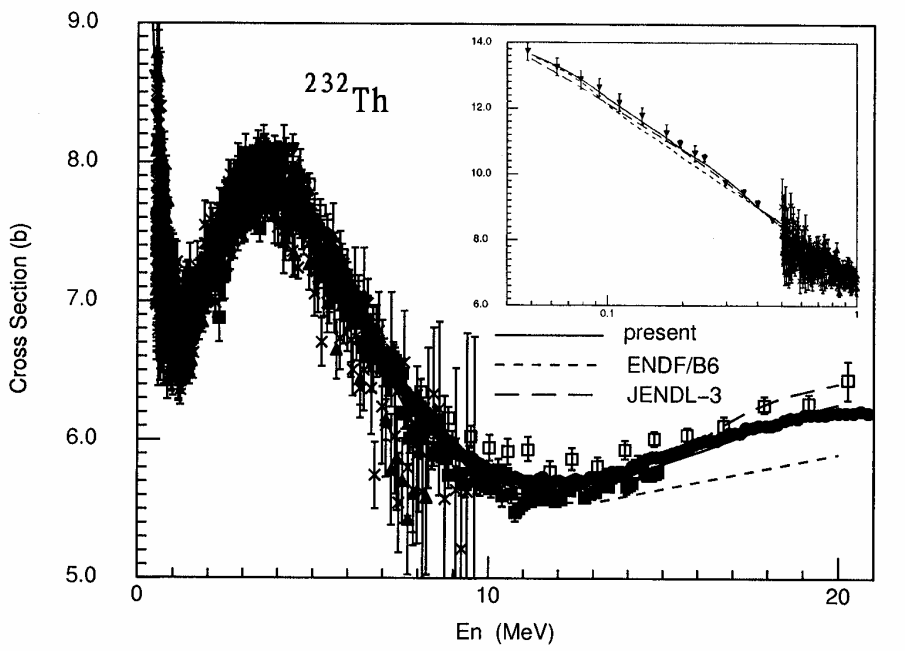

Fig.1 Calculated neutron total cross sections compared with experimental data.

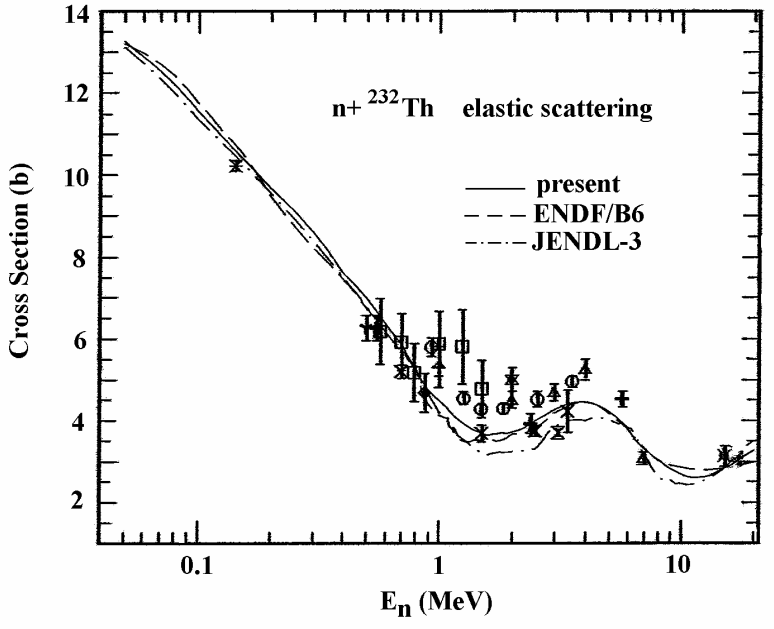

Fig.2 Calculated neutron elastic scattering cross section compared with experimental data.

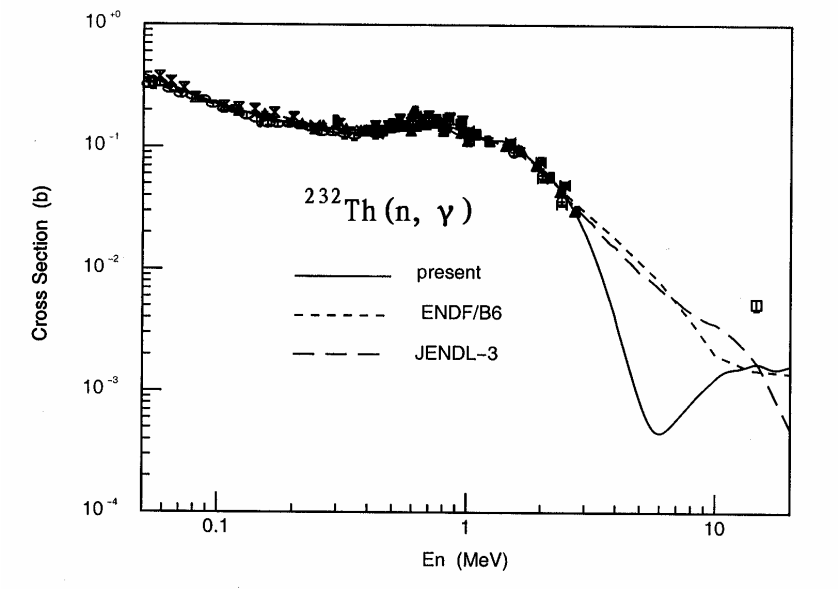

Fig.3 Calculated neutron captures cross section compared with experimental data.

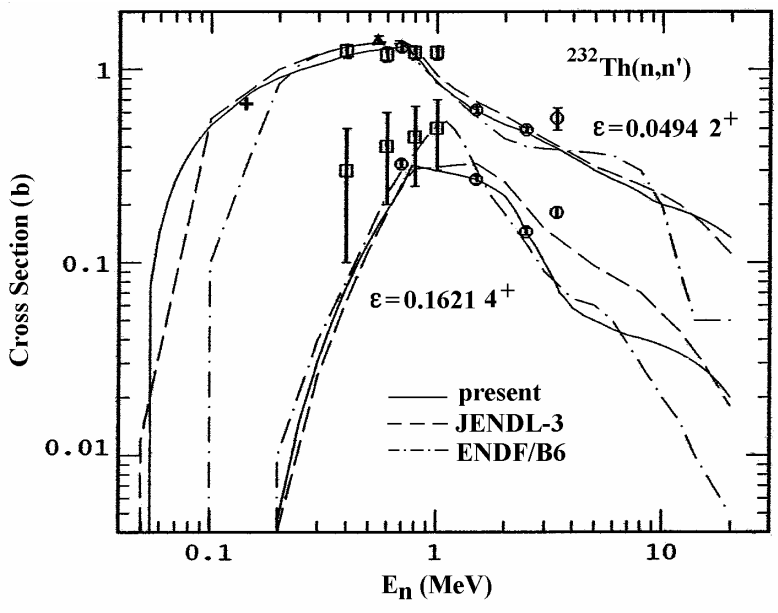

Fig.4 Calculated neutron inelastic cross section for the first and second excited levels compared with experimental data.

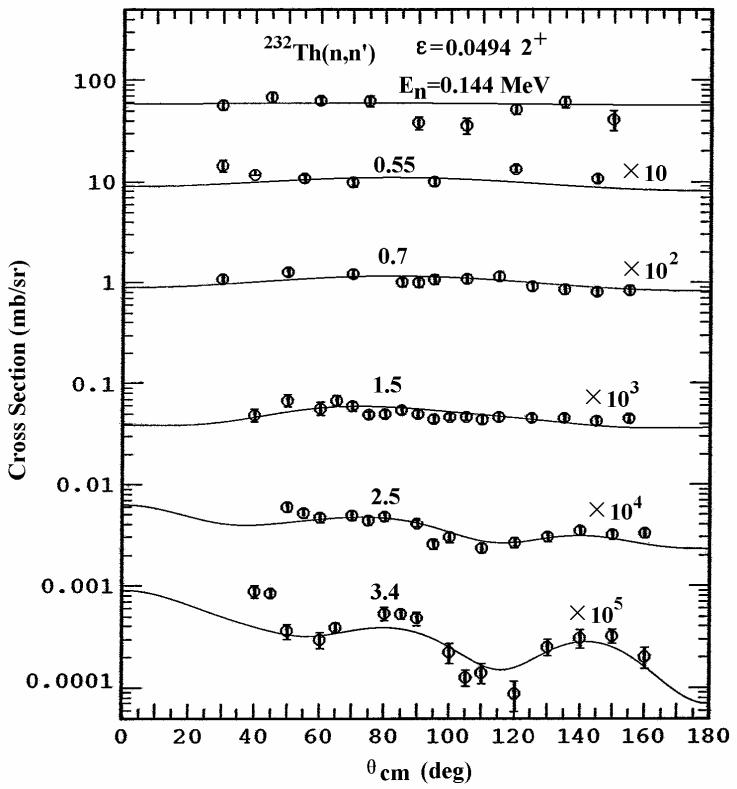

Fig.5 Calculated neutron inelastic scattering angular distribution for the first excited level compared with experimental data.

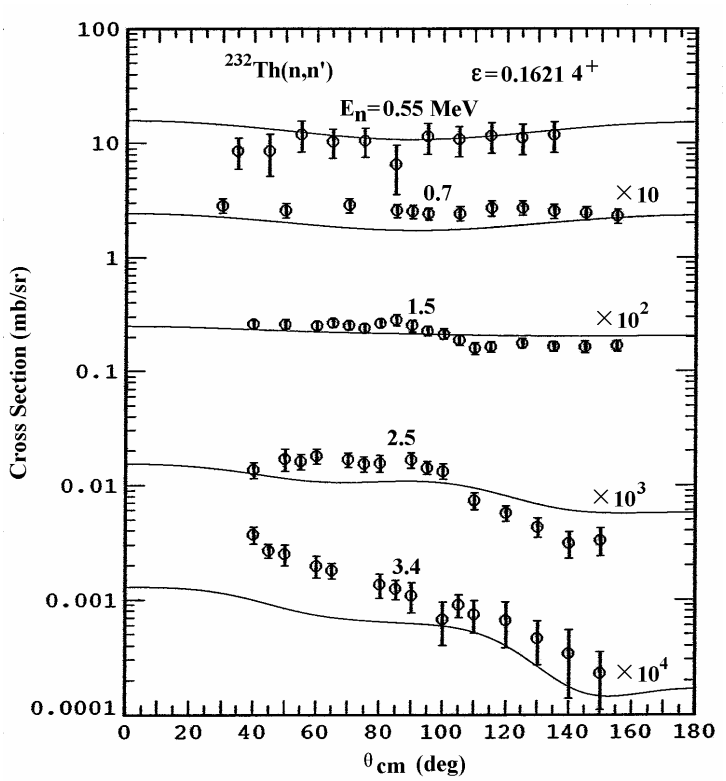

Fig.6 Calculated neutron inelastic scattering angular distribution for the second excited level compared with experimental data.

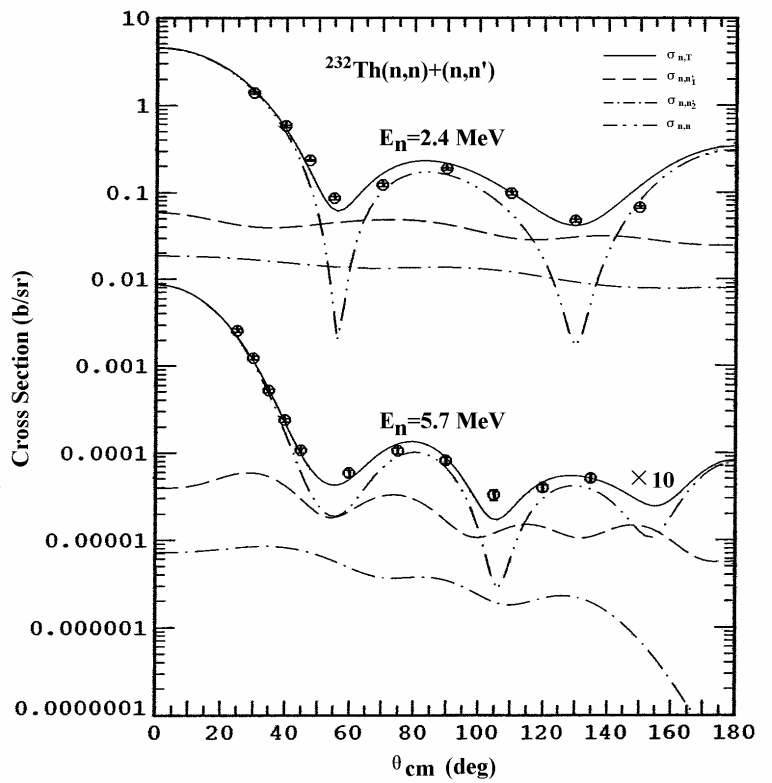

Fig.7 Calculated neutron elastic and inelastic scattering angular distribution of the first and second excited levels compared with experimental data at energy 2.4 and 5.7 MeV.

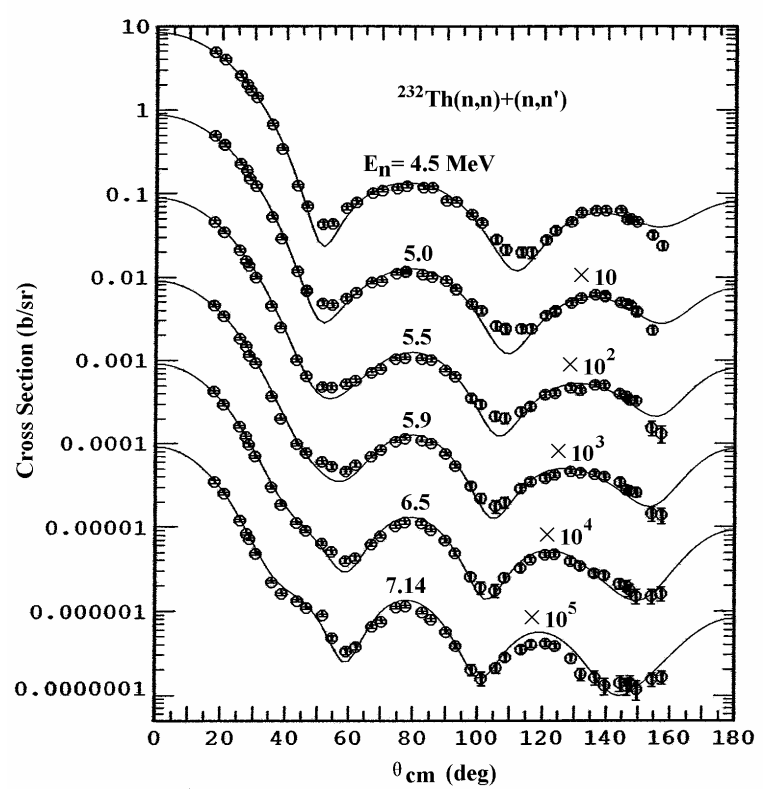

Fig.8(a) Calculated neutron elastic and inelastic scattering angular distribution of the first, second and third excited levels compared with experimental data.

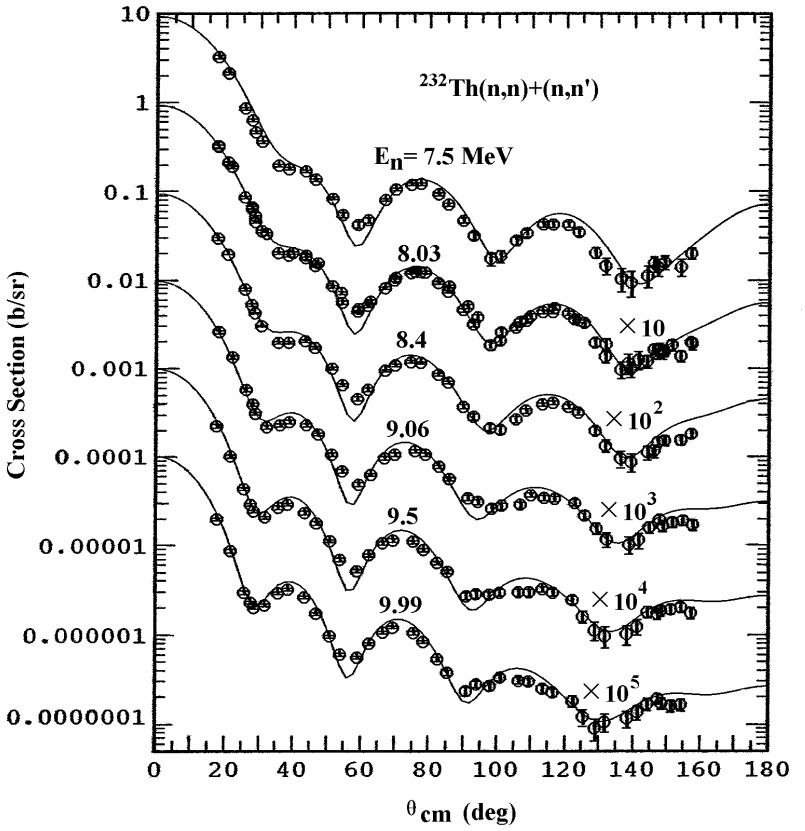

Fig.8(b) Calculated neutron elastic and inelastic scattering angular distribution of the first, second and third excited levels compared with experimental data.

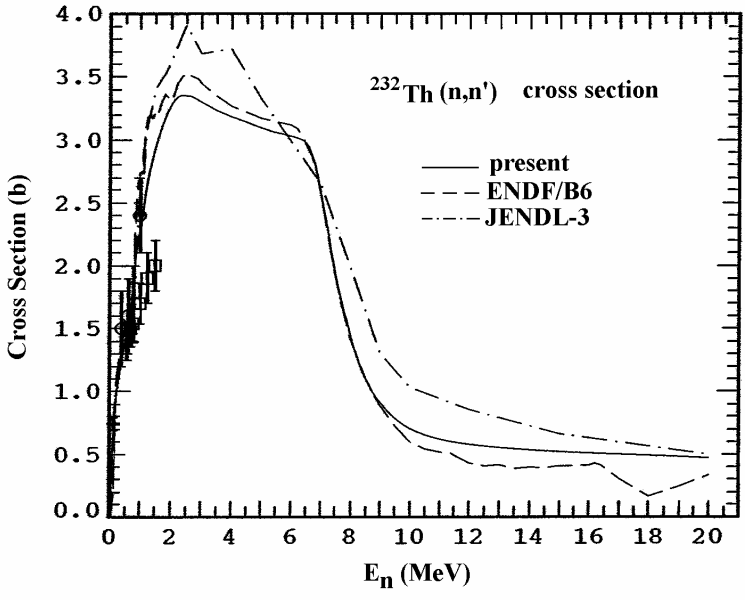

Fig.9 Calculated neutron inelastic cross sections compared with experimental data.

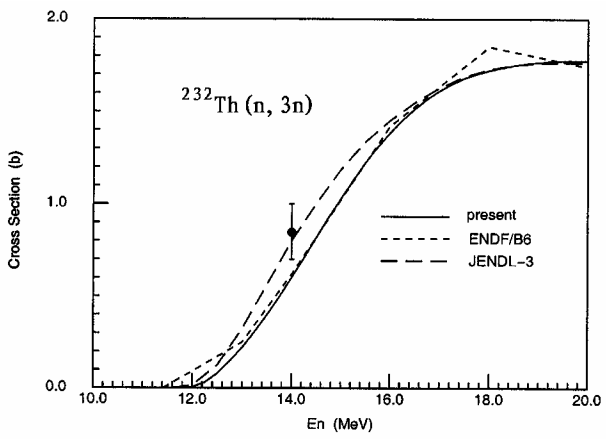

Fig.10 Calculated (n, 3n) reaction cross sections compared with experimental data.

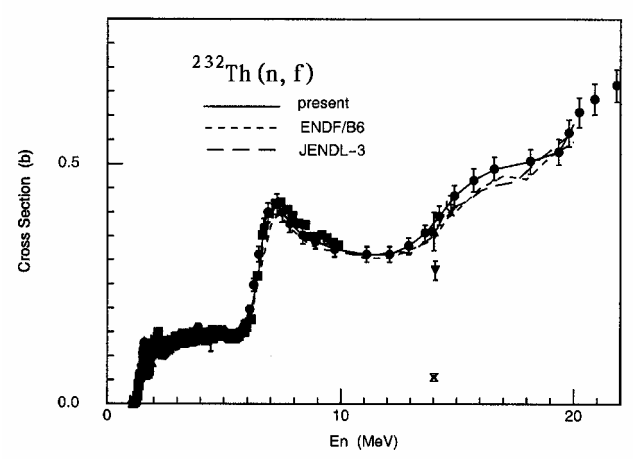

Fig.11 Calculated neutron fission cross sections compared with experimental data.

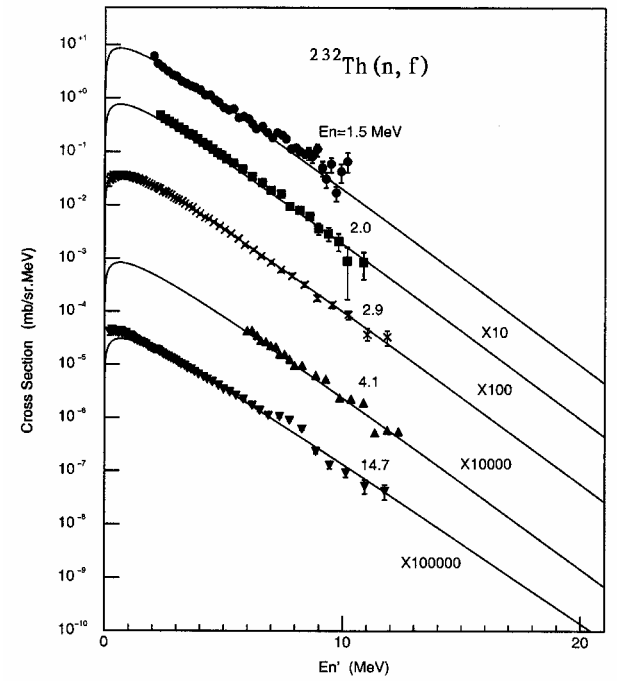

Fig.12 Calculated neutron fission spectra compared with experimental data at 1.5, 2.0, 2.9, 4.1 and 14.7 MeV incident neutron energy.

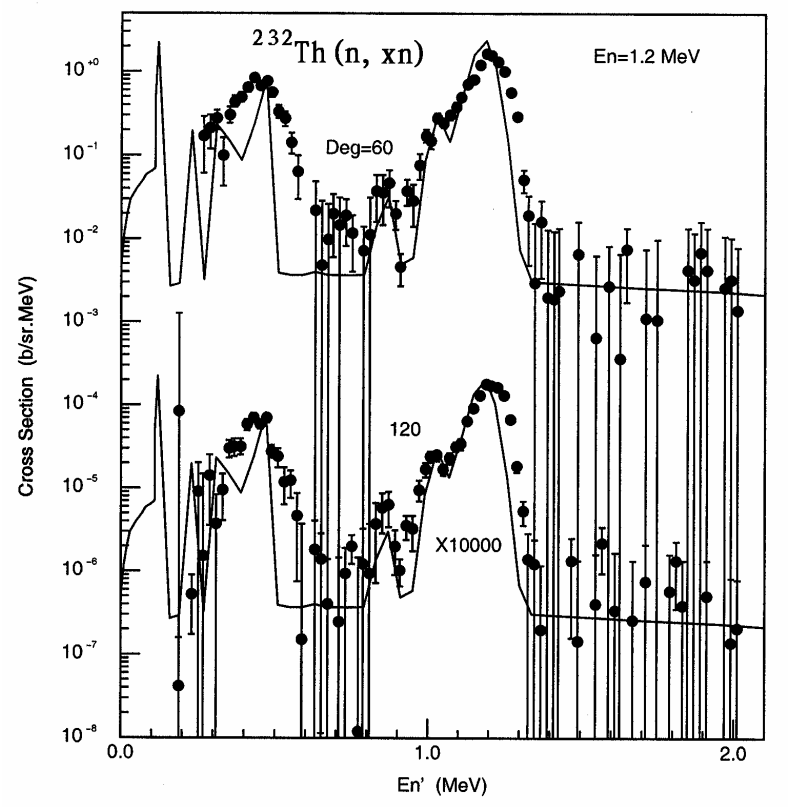

Fig. 13 Calculated double differential neutron emission spectra compared with experimental data at 1.2 MeV incident energy.

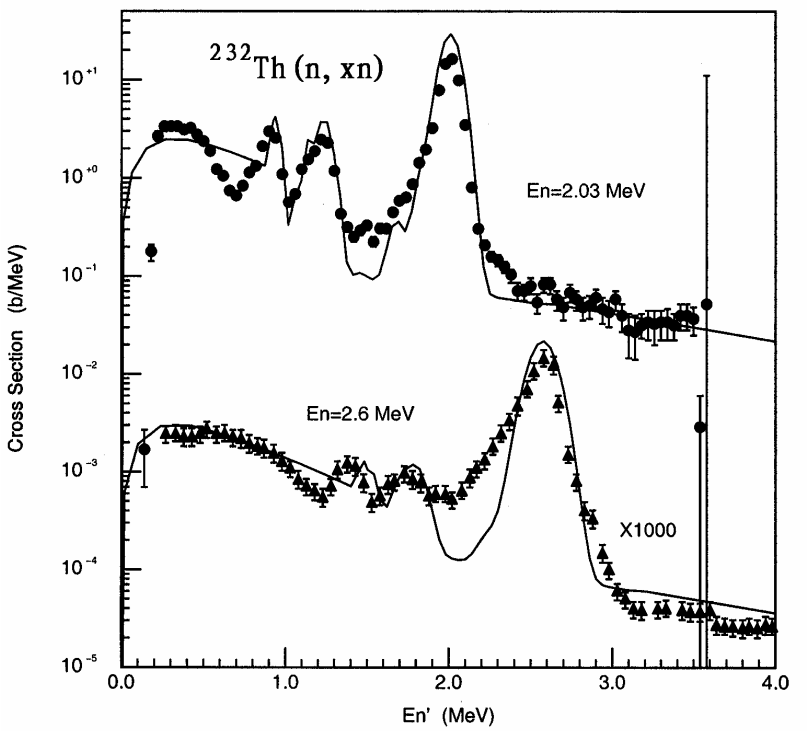

Fig.14 Calculated angle-integrated neutron emission spectra compared with experimental data at 2.03 and 2.6 MeV incident energy.

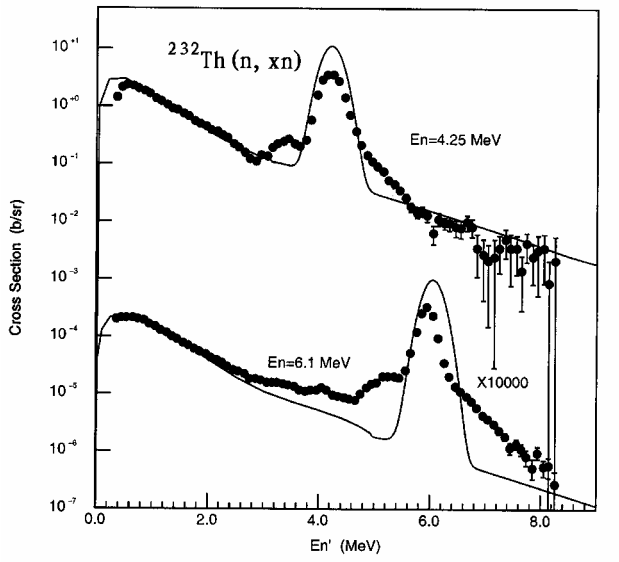

Fig.15 Calculated angle-integrated neutron emission spectra compared with experimental data at 4.25 and 6.1 MeV incident energy.

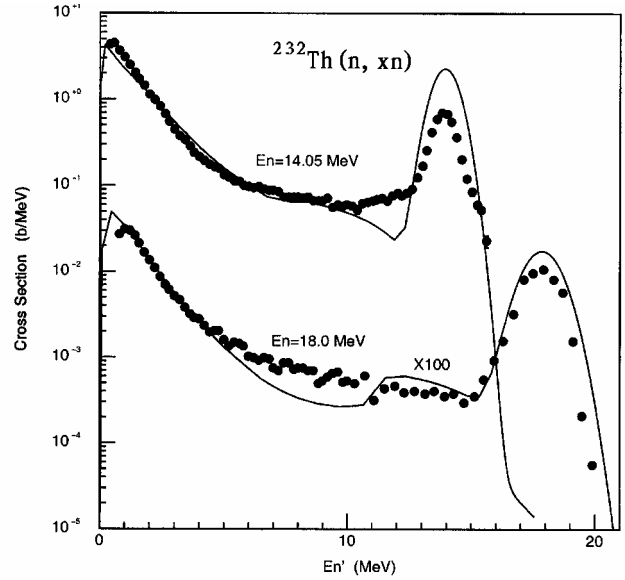

Fig.16 Calculated angle-integrated neutron emission spectra compared with experimental data at 14.05 and 18.0 MeV incident energy.

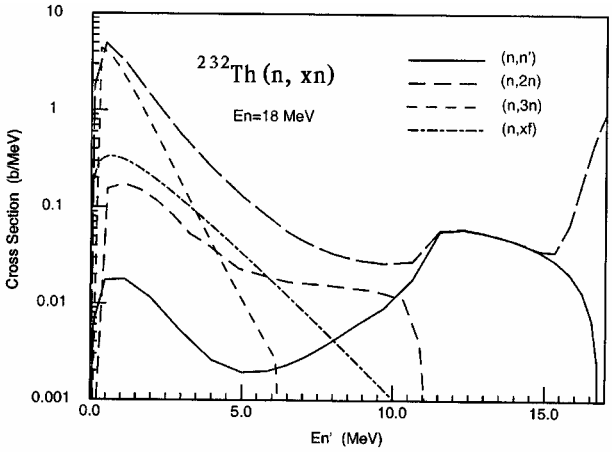

Fig.17 Calculated angle-integrated neutron emission spectra at 18.0 MeV incident energy.